



SPECTRUM CHARACTERISTICS OF SEISMOGRAMS and RELATIVE AMPLIFICATIONS in the MeSO-net

- An effect on investigation of attenuation structures -

R. Nakamura⁽¹⁾, S. Sakai⁽²⁾, H. Tsuruoka⁽³⁾, A. Kato⁽⁴⁾, N. Hirata⁽⁵⁾, T. Shiina⁽⁶⁾

⁽¹⁾ Project researcher, Earthquake Research Institute, The University of Tokyo, naka@eri.u-tokyo.ac.jp

⁽²⁾ Associate professor, Earthquake Research Institute, The University of Tokyo, coco@eri.u-tokyo.ac.jp

⁽³⁾ Associate professor, Earthquake Research Institute, The University of Tokyo, tsuru@eri.u-tokyo.ac.jp

⁽⁴⁾ Professor, Earthquake Research Institute, The University of Tokyo, akato@eri.u-tokyo.ac.jp

⁽⁵⁾ Professor, Earthquake Research Institute, The University of Tokyo, hirata@eri.u-tokyo.ac.jp

⁽⁶⁾ Project researcher, Earthquake Research Institute, The University of Tokyo, t-shiina@eri.u-tokyo.ac.jp

Abstract

In the Kanto district, Japan, a dense seismograph network, called as the Metropolitan Seismic Observation network (MeSO-net) [1], has been deployed. The MeSO-net consists of around 300 accelerometers. Since accelerometers of the MeSO-net, K-NET, and KiK-net are densely distributed in the Kanto district, an integrated data analysis from these networks will be able to improve understanding of the strong motion and structural heterogeneity in and around the metropolitan area of Japan. The K-NET and some of the KiK-net stations are installed at the ground surface, whereas the MeSO-net stations are installed at a depth of 20 m. Therefore, it is important to investigate the response of the MeSO-net to seismic waves (relative to the ground surface stations) in order to integrate analysis of multiple seismic networks.

In this study, we first outline the works by Nakamura et al. [2] who estimated relative site amplification factors of the MeSO-net stations by improving the method of Ikeura and Kato [3]. Second, we explore effects of the prior constrains of site amplification factors on estimations of three-dimensional S-wave attenuation structure in the Kanto district.

For estimating the relative site amplification factors, we built a station network of station pairs less than 10 km apart. We calculated the relative amplifications of the MeSO-net stations, referencing site amplifications of ground stations of the K-NET and the KiK-net. The relative amplification factors were determined using least squares fitting by the Algebraic Reconstruction Technique with Bayesian constraints (ARTB) method [4]. The Fourier spectral amplitude was compared every 1 Hz from 1 Hz to 10 Hz. We selected strong motion records by the MeSO-net from 2011 to 2015, and by K-NET/KiK-net from 1996 to 2016. A total of 962,422 station pairs were selected from 394 stations, including 297 MeSO-net stations.

Furthermore, we examined the effectiveness of prior constraints of site amplification factors on three-dimensional attenuation inversion. Generally, there is a trade-off between site amplification factors and attenuation structures. To mitigate this trade-off, previous studies [5-8] divided the stations into several groups based on the PS logging data and assumed that amplification factors were constant within each station group. By adopting the given amplification factors, we observed that the residuals with respect to S-wave attenuation were smaller than that of the previous method, in which amplification factors were estimated simultaneously with the attenuation structure. These results suggest that our approach reducing influences of the trade-off between the attenuation structures and the site amplification is effective in obtaining a three-dimensional attenuation structure.

Keywords: Metropolitan Seismic Observation network (MeSO-net); Relative site amplification factor; strong motion seismogram, S-wave attenuation

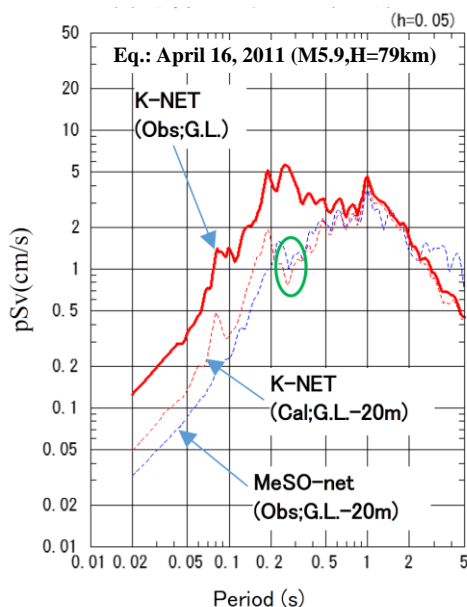
1. Introduction

In the Kanto district, Japan, the Metropolitan Seismic Observation network (MeSO-net) [1], has been operated. The station network includes approximately 300 accelerometers and has been collecting waveforms since 2008. In the MeSO-net, seismometers are installed approximately 20 m beneath the ground surface to reduce near-surface noise from human activities. These MeSO-net stations cover the entire this region. In addition, accelerometers for strong ground motion are distributed on the ground surface (e.g., the K-NET and KiK-net)

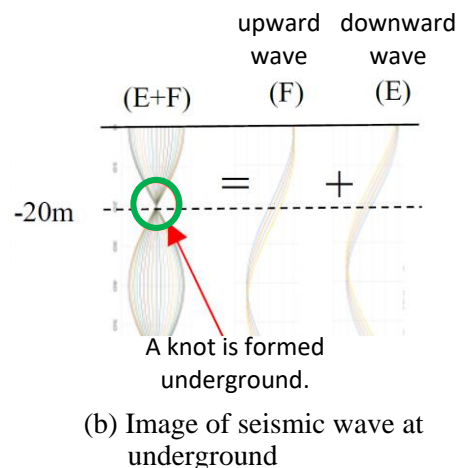


in the Kanto district. Thus, analysis of the observational data from these high-density and high-sensitivity seismograph networks will provide a unique opportunity for precise estimation of the three-dimensional structure and seismic wave propagation processes. However, the MeSO-net records probably show site amplifications different from those of the K-NET/KiK-net records, because the seismometers of MeSO-net are installed within the ground. Therefore, it is necessary to evaluate seismic response of the MeSO-net for integrated analysis with K-NET/KiK-net.

Nakamura et al. [9] reported the presence of troughs in the spectrum seismograms obtained at the MeSO-net stations. The trough would be attributed to superpositions of the upgoing and downgoing waves at the seismometer installed in the ground. The response spectra of the MeSO-net (E.OA5M) and the K-NET (TKY007) stations (installed beneath and at the ground surface, respectively) are plotted as red solid and blue dashed lines in Fig. 1(a), respectively. Note that the distance between stations is only 0.7 km, but the spectral amplitudes are clearly different between the two sites. Nakamura et al. [9] calculated a virtual response spectrum at a depth of 20 m below ground level (G.L.) (red dotted line in Fig.1(a)) assuming the PS logging data obtained at the K-NET station (TKY007). The dominant period of the 1st mode (on the ground surface) is predicted to be around 0.3 s based on the logging data. This specific period well coincides with a local trough of spectrum amplitude of the observed waveform in MeSO-net (approximately 0.3 s) (indicated by the green circle in the figure).



(a) Response Spectrum ($h=5\%$)
MeSO-net: E.OA5M station
K-NET: TKY007 (Shinjuku)



(b) Image of seismic wave at underground

Fig.1 Example of the trough on spectrum formed due to underground installation of seismograph [9].

Nakamura et al. [9] also investigated the amplification at the MeSO-net and the K-NET/KiK-net stations simultaneously with the three-dimensional attenuation structure. Based on the average S-wave velocity up to a depth of 30 m (AVS30) estimated by National Research Institute for Earth Science and Disaster Resilience (NIED), these stations were categorized into ten groups: two groups for the MeSO-net and eight groups for the K-NET/KiK-net stations. However, in the result of their study, the obtained seismic response of individual station groups may be few to precisely separate effects of amplification factor from seismic attenuation structure, because the MeSO-net stations were divided into only two groups: soft and hard soil conditions.

Furthermore, Nakamura et al. [2] studied the amplification factor of the MeSO-net station relative to K-NET and KiK-net stations by using Ikeura and Kato's method [3]. This approach could determine the



amplification factors independently from attenuation structures. In the present study, we will show the advantages of the prior determination of the relative amplification factor on the study of the three-dimensional attenuation structure.

2. Relative amplification factors

Nakamura et al. [2] investigated the relative amplification factors among the MeSO-net stations. Here, we briefly describe the method and data used in the present study, showing the obtained relative amplification factors of the MeSO-net stations.

2.1 Methods and data

We consider that seismograms for an earthquake are obtained at two nearby stations. Since radiation patterns and propagation effects are almost the same, differences in the seismograms would reflect variations in the site amplification factors. Borchardt [10], Fujimoto and Midorikawa [11] and Ikeura and Kato [3] have already developed a method to estimate relative amplification factors based on this principle. Each study computed an amplification factor from the spectral ratio of seismograms recorded at adjacent stations. However, seismic stations are not exactly located at the same position, indicating that the inter-station distance is an important index for canceling out the radiation characteristics and propagation effects from the spectral ratio. Borchardt [10] and Fujimoto and Midorikawa [11] computed the spectral ratio observed at a station pair within an inter-station distance of 30 km. Ikeura and Kato [3] constructed a station network in which the maximum inter-station distance was 25 km and estimated the relative amplification factor around the Tohoku Pacific coast using least squares fitting.

Nakamura et al. [2] improved the approach of Ikeura and Kato [3] and estimated the relative amplification factors among the MeSO-net, K-NET and KiK-net stations (Fig. 2(a)). The inter-station distance of 10 km or less was adopted for the station pair selection. The ARTB method [4] was used, as the least squares method can efficiently determine the model parameter (here, the relative amplification factor).

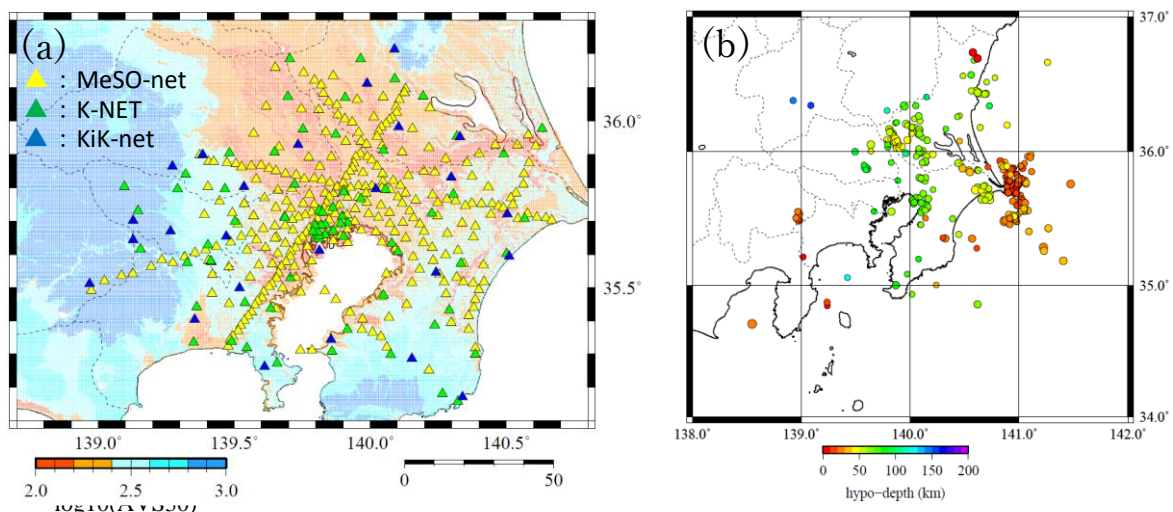


Fig.2 Distributions of (a) stations and (b) earthquakes. Background of (a) is AVS30 of J-SHIS (Japan Seismic Hazard Information Station [2]).



We collected seismograms from the MeSO-net (from 2011 to 2015), and K-NET/KiK-net (from the beginning of those station networks to July 2016). We used seismograms for earthquakes with magnitudes of earthquakes were M_j (determined by Japan Meteorological Agency: JMA) of 4.0 or greater and depths shallower than 200 km (Fig. 2(b)). We analyzed the NS component seismograms in this study, but we excluded the seismograms of which amplitude was greater than 100 Gal in order to minimize nonlinear effects due to strong ground motion. As a result, we determined amplification factors of 394 stations, including 297 MeSO-net stations, from a total of 962,422 station pairs.

The ratio of the spectrum amplitude calculated for i -th and j -th stations, d_{ij} , is expressed as

$$d_{ij}(f) = \log \left(\frac{O_i(f)}{O_j(f)} \right) = \log O_i(f) - \log O_j(f),$$

where O is the observed spectrum amplitude after corrected geometrical spreading effects, f is the frequency. Here, the observation equation, $\mathbf{d} = \mathbf{G}\mathbf{m}$, is described below,

$$\begin{bmatrix} d_{12}(f) \\ d_{13}(f) \\ \vdots \\ d_{(n-1)n}(f) \end{bmatrix} = \begin{bmatrix} 1 & -1 & 0 & \cdots & 0 & 0 \\ 1 & 0 & -1 & \cdots & 0 & 0 \\ \vdots & \vdots & \vdots & \ddots & \vdots & \vdots \\ 0 & 0 & 0 & \cdots & 1 & -1 \end{bmatrix} \begin{bmatrix} m_1(f) \\ m_2(f) \\ m_3(f) \\ \vdots \\ m_{n-1}(f) \\ m_n(f) \end{bmatrix},$$

where m represents the amplification factor, and n is the number of stations. the ARTB method [4] was used to solve this observational equation and estimated relative values of m .

2.2 Numerical Experiments

Numerical experiments were performed to evaluate the reliability of the obtained results. In the numerical experiment, we computed synthetic amplification factors giving the perturbations of $10^{0.5}$ (≈ 3.16) and $10^{-0.5}$ (≈ 0.316) to the initial values alternatively (Fig. 3(a)). We then inverted the synthetic data and verified how well the synthetic model is recovered.

The amplification factor of $10^0 (= 1)$ is set as the initial value in all stations, and 50 iterations were performed. The imposed amplification factors were approximately recovered after only one iteration (Fig. 3); however, large residuals remained in peripheral regions of the study area (Fig. 4(a)). As shown in Figs. 4(b) and 5, the assumed amplification factors were finally recovered after 50 iterations.

2.3 Results of the relative Amplifications

From the results of numerical experiments, the exact characteristics in the site amplification factors of the station network could be determined after 50 iterations in this study. For satisfactory analysis, we performed 100 iterations for analysis of the observational data.

Fig. 6 shows a comparison of the results at stations of the K-NET and KiK-net at ground surfaces. The obtained amplification factors are grouped by the AVS20 based on PS logging at depths of 0-20 m. The average amplification factors in each AVS20-groups are compared in Fig.6(f), indicating the amplification factors tend to increase at the station group with small AVS20. On the other hand, Fig. 6(e) displays that the reference station IBRH19 (Tsukuba) mark the larger amplifications at 3-6 Hz than station SIT012 (Hanno) and TKYH13 (Hagiwara Minami), which belong to the same AVS20-group. These slight variations in amplification factors may reflect different subsurface structures just beneath the stations.

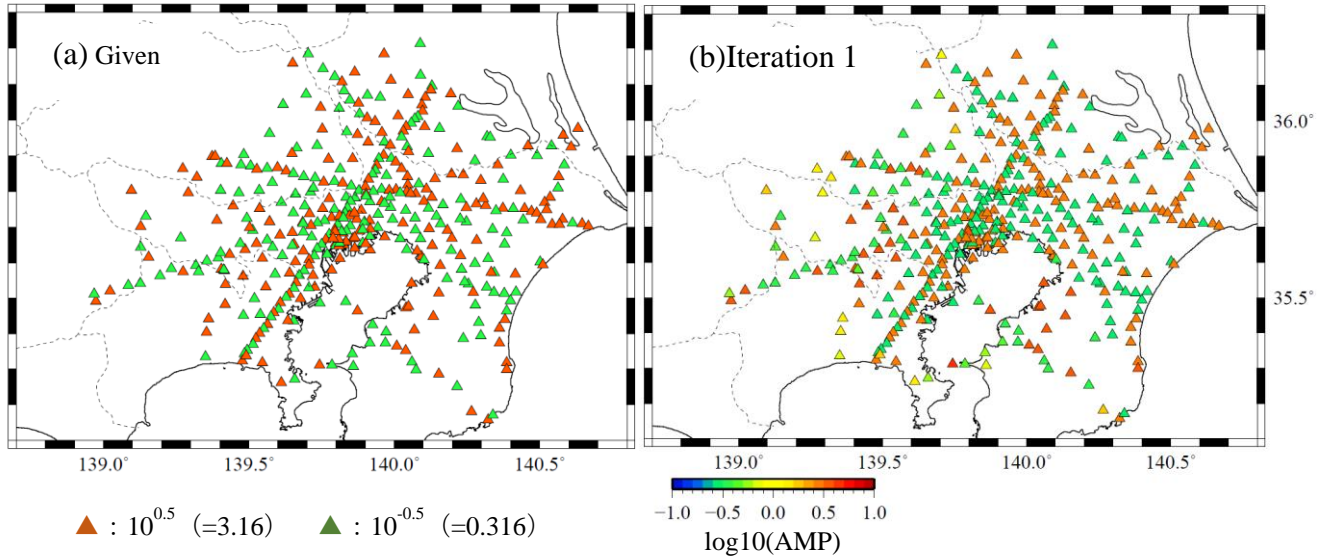


Fig. 3 Numerical experiment. (a) given amplification. (b) recovered amplification after the first iteration [2].

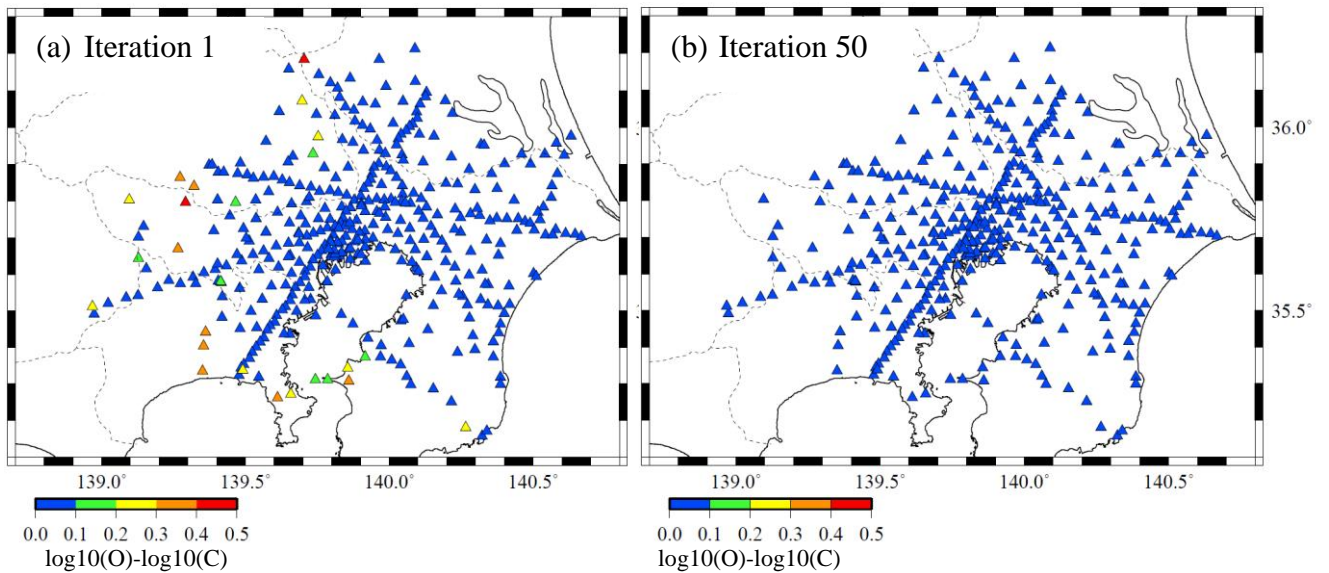


Fig. 4 Distribution of residuals by numerical experiment (a) after one iteration and (b) after 50 iterations. [2].

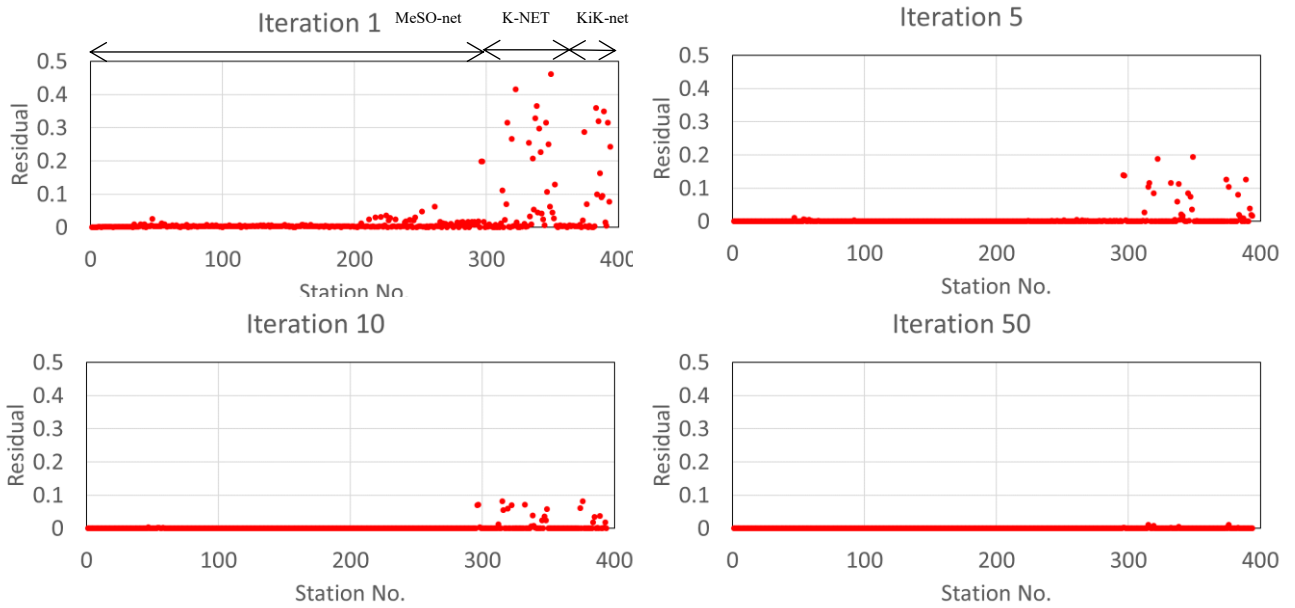


Fig. 5 Residuals at each observation station [2].
(No.1-298:MeSO-net, No.299-369:K-NET, No.370~394 : KiK-net)

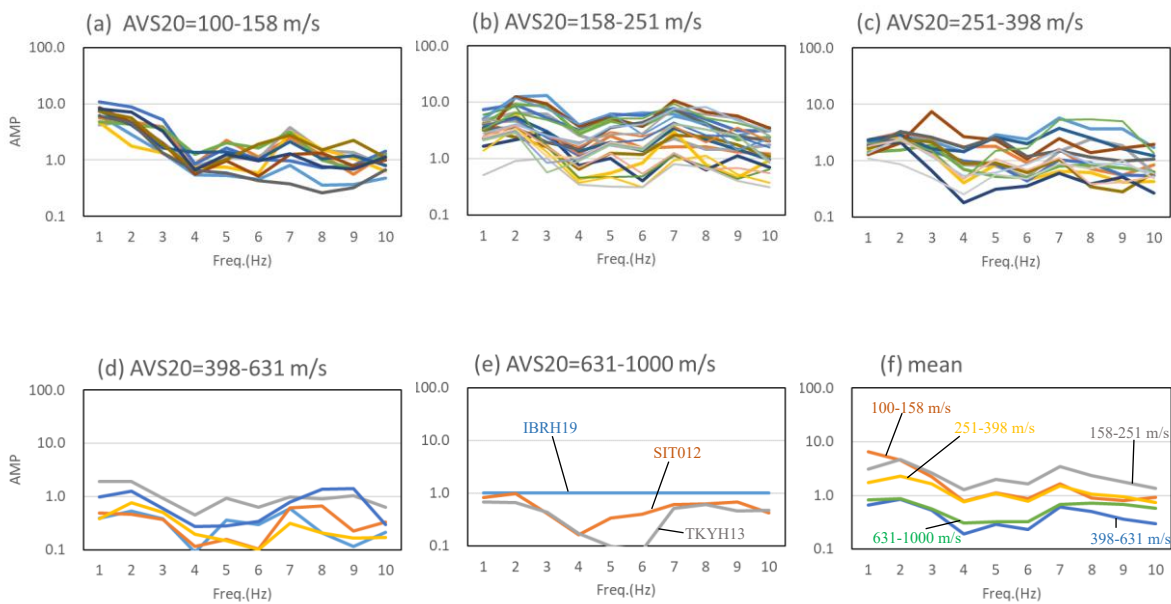


Fig. 6 Amplification of K-NET and KiK-net (at ground) with IBRH19 (Tsukuba) as reference station [2]. AVS20 is based on PS logging (depth 0-20m).

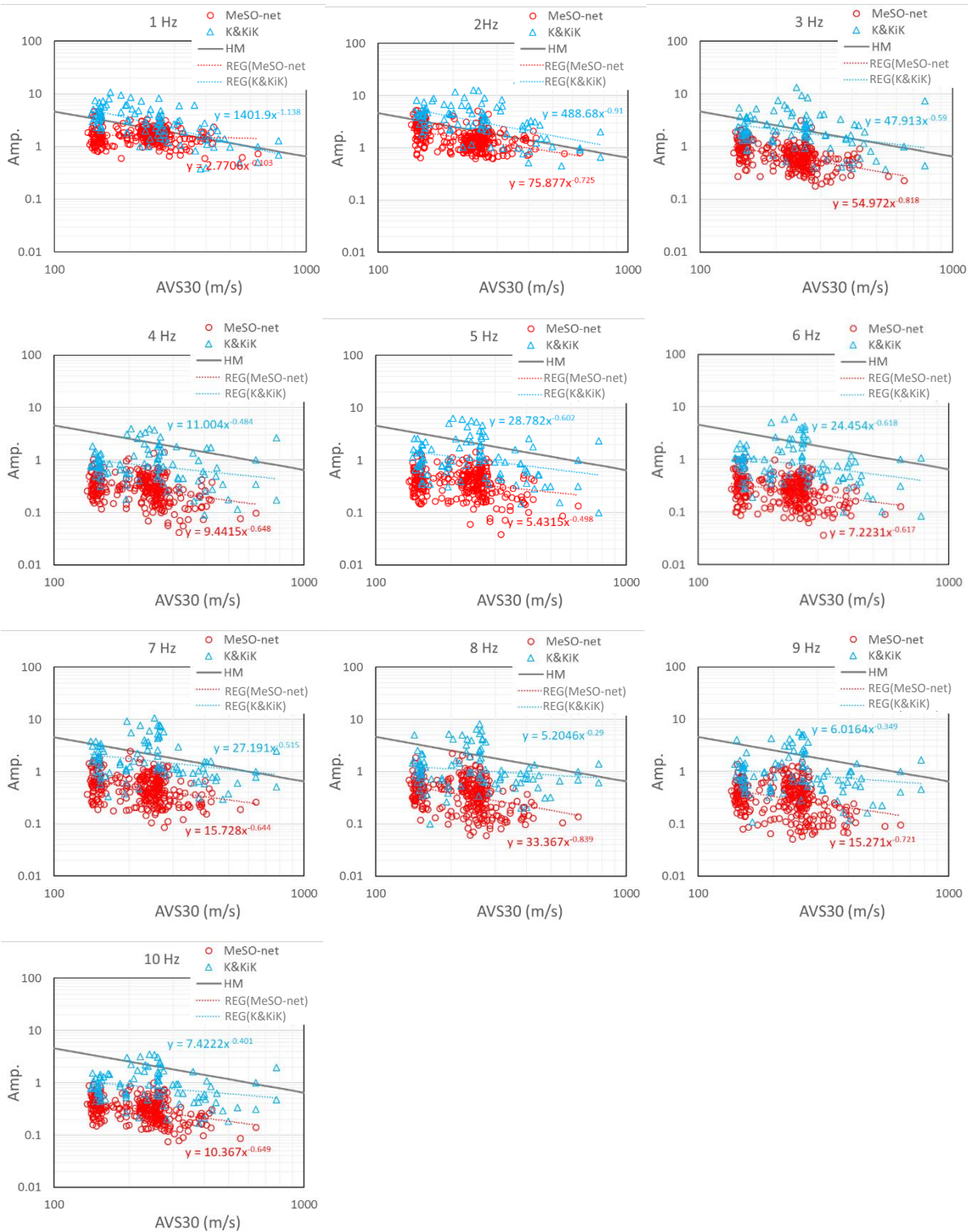


Fig.7 Comparison between AVS30 and relative amplification factors [2]. AVS30 is based on J-SHIS[1]250m mesh data. Reference station IBRH19 was set to 1.0. HM : amplification for PGV obtained by Fujimoto and Midorikawa [11], REG: regression.

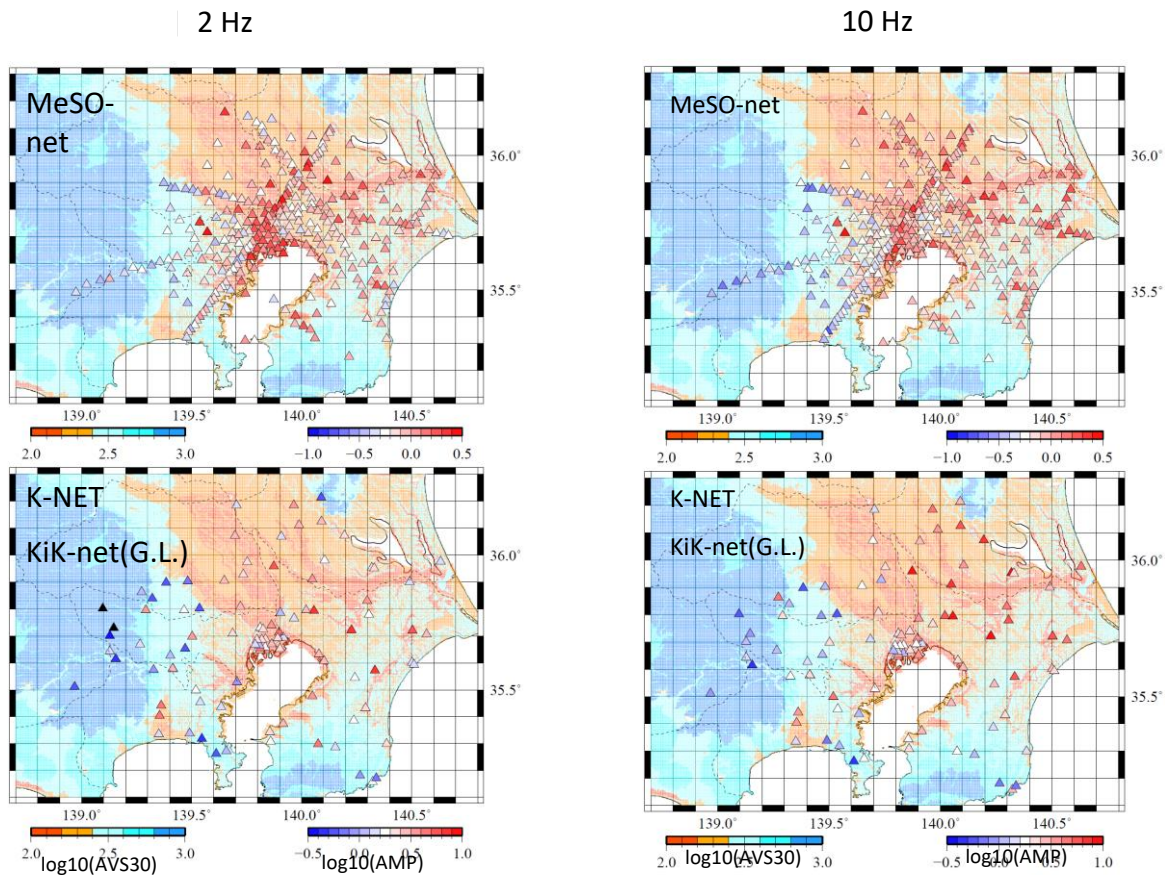


Fig.8 Distribution of relative amplification factor at 2 Hz and 10Hz superimposed on AVS30 of J-SHIS [2].

The obtained amplification factors of the MeSO-net, K-NET, and KiK-net stations are plotted over AVS30 of J-SHIS as shown in Fig.7. The amplification factors estimated at a frequency higher than 3 Hz are about 3 times larger at the ground surface stations (K-NET and KiK-net) than those of the MeSO-net stations, whereas those differences in 1-2 Hz are small. In all of the frequency range, the variations in the amplification factors decrease with increasing the AVS30 values, coinciding the trend with the amplification of peak ground velocity (PGV) expected in Fujimoto and Midorikawa [11]. The well-matched spatial distributions of amplification factors to the AVS30 are also seen in Fig. 8.

3. Estimations of three-dimensional attenuation structure considering the relative amplification factors

In the exploration of three-dimensional attenuation structure, there is a trade-off between site amplification and spatial variation in attenuation, generally expressed as the quality factor (Q). To reduce ambiguity due to this trade-off, Nakamura and Uetake [5], Nakamura et al. [6], Nakamura [7] and Nakamura and Shiina [8] divided stations into several groups based on the PS logging data and treated the site amplification factor in



each station group as the same constant value. The dominant frequency of amplification for each group obtained by simultaneous inversion were concordant with those calculated from PS logging data [5,7]. This mean that the simultaneous inversion considering the several grouping amplifications is effective to minimize the trade off with attenuation structure. Meanwhile, exactly considering amplification at individual station may provide further detailed information for the attenuation structure.

Therefore, we performed the two cases for inversions of three-dimensional attenuation structures. The first case followed the previous studies [9]: the K-NET and KiK-net stations were divided into 8 groups and the MeSO-net stations into 2 groups. The second case is the new approach proposed in this study: the amplification factor estimated by Nakamura et al. [2] was fixed in the inversion process. The other calculation conditions were the same as the previous study [9]; that is, the block size was set to be $0.1^\circ \times 0.1^\circ \times 10$ km.

The residuals clearly decreased by a priori constraints the site amplification factors on inversion (Fig.9). The final residuals at 10 Hz in the first and the second cases are 0.46 and 0.43, respectively: about 10 % of the residuals are improved. Since the attenuation structures and site amplification factors are estimated in the first case, the number of unknown model parameters is larger than that of the second case. However, the residuals of the second case are generally small, meaning that the inversion adopting prior constrained relative amplifications of the stations, namely the second case in this study, is effective in an inversion of the three-dimensional attenuation structures.

The obtained attenuation structures are shown in Fig.10. There are differences between Case 1 and Case 2 results. For example, in Case 2, high values are continuously obtained from 20 km to 50 km in the southwestern part (near Kanagawa Prefecture) of the figure, whereas in Case 1, they do not seem to be continuous. We will expand the calculation area on the attenuation structure and study its interpretation in the future.

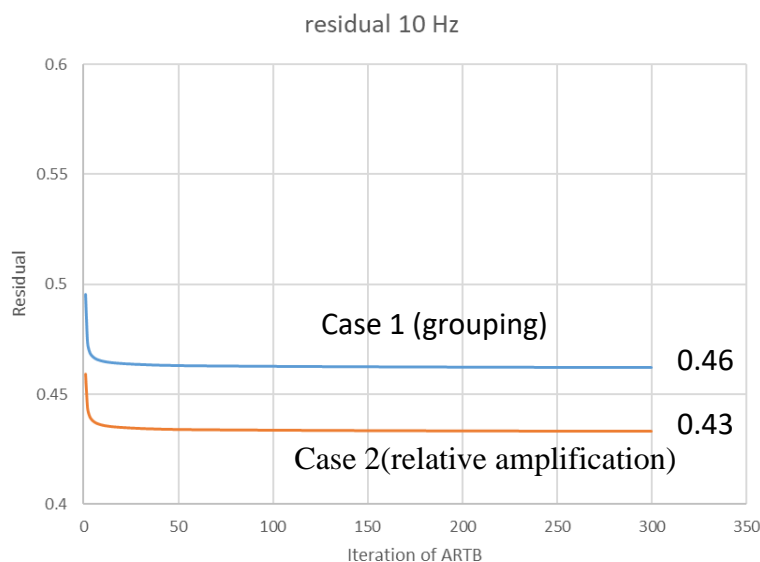


Fig.9 Residuals comparing relative amplification case and grouping case.

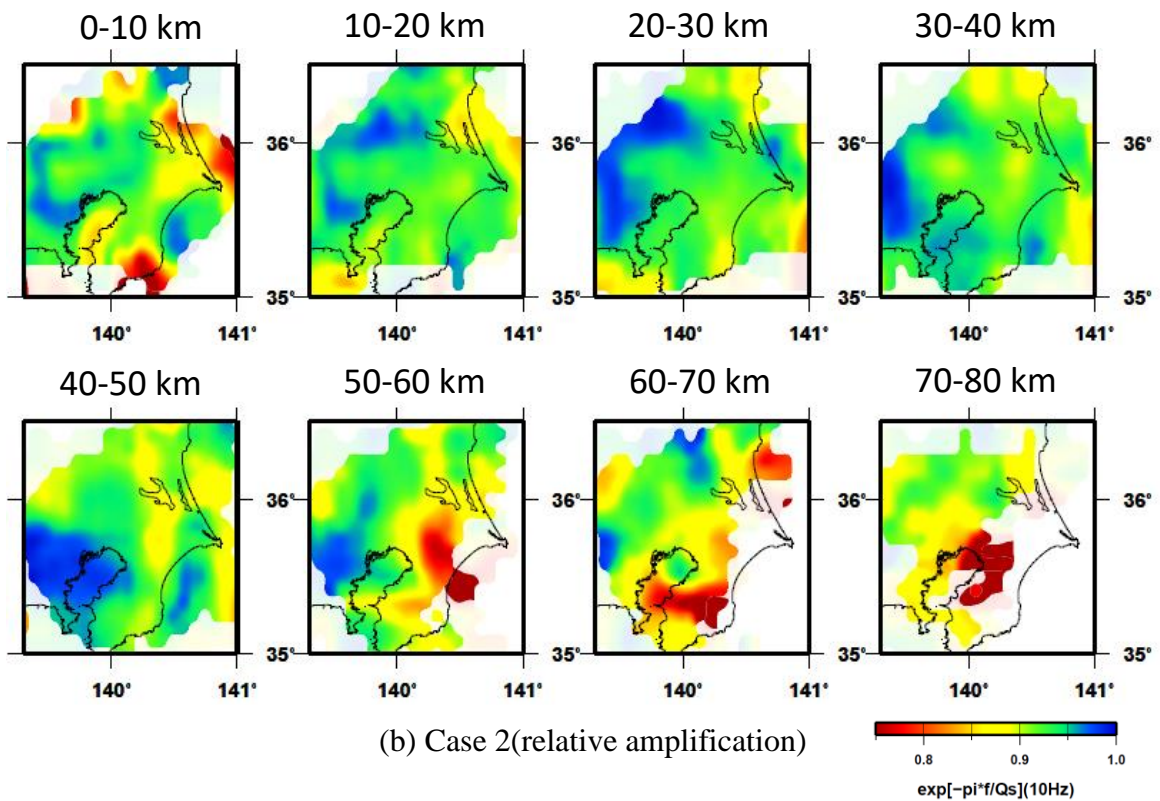
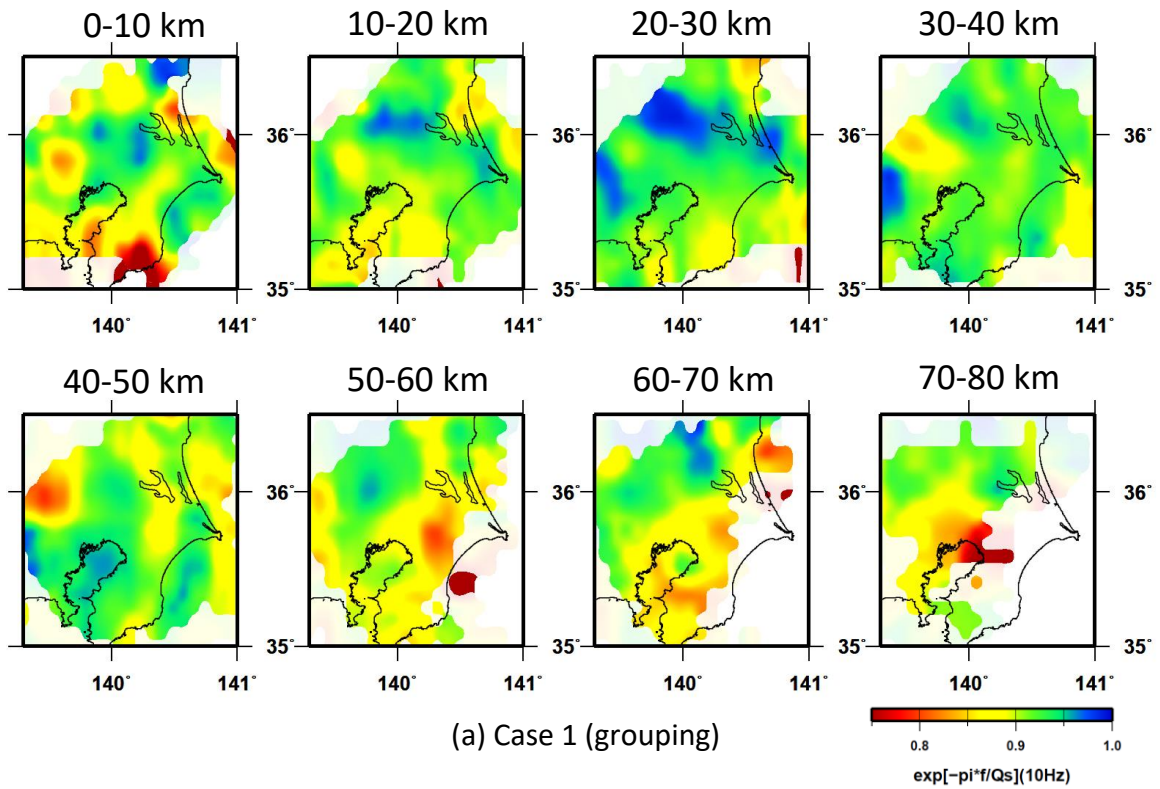


Fig.10 Three dimensional Q_s structure on (a) Case 1 [grouping] and (b) Case 2 [relative amplification]. The well-resolved areas are displayed: the areas where the restoration index RI [8] is greater than 0.001 are masked.



5. Acknowledgments

We used K-NET and KiK-net data of the National Research Institute for Earth Science and Disaster Resilience (NIED). Dr. Senna in NIED gave us valuable feedback. This research was supported by the Ministry of Education, Culture, Sports, Science and Technology commissioned research “Resilience Comprehensive Strength Improvement Project Centered in the Tokyo Metropolitan Area” and was partially supported by JST, CREST (JPMJCR1763). Some figures are made by the GMT software [12].

6. References

- [1] Kasahara K, Sakai S, Morita Y, Hirata N, Tsuruoka H, Nakagawa S, Nanjo K, Obara K (2009): Development of the Metropolitan Seismic Observation network (MeSO-net) for detection of mega-thrust beneath Tokyo Metropolitan Area, *Bulletin of the Earthquake Research Institute, The University of Tokyo*, **84**(2), 71-88. (in Japanese with English Abstract) <http://hdl.handle.net/2261/33038>
- [2] Nakamura R, Sakai S, Tsuruoka H, Kato A, Hirata N, Shiina T (2019): Relative Amplification on MeSO-net Installed Underground and K-NET/KiK-net Installed Surface Ground, *abstract of JAEE annual meeting*, **P1-12**, 1-10. (in Japanese)
- [3] Ikeura T. and Kato K (2011): Evaluation of relative site amplification factors by combining average spectral ratios of strong motions simultaneously observed at adjacent two sites -Amplification to K-NET and KiK-net sites in the Pacific coast side of the Tohoku district -, *The Journal of JAEE*, 11, 48-67. (in Japanese with English Abstract) https://doi.org/10.5610/jaee.11.4_48
- [4] Herman GT (1980): Image reconstruction from projections: The fundamentals of computerized tomography, *Academic Press*, New York, 316.
- [5] Nakamura R, Uetake T (2002): Three dimensional attenuation structure and site amplification inversion by using a large quantity of seismic strong motion records in Japan, *Zisin*, 54, 475-488, (in Japanese with English Abstract) , https://doi.org/10.4294/zisin1948.54.4_475
- [6] Nakamura R, Satake K, Toda S, Uetake T and Kamiya S (2006): 3-D Attenuation Structure beneath the Kanto District, Japan, *Geophys. Res. Lett.*, L21604. <https://doi.org/10.1029/2006GL027352>
- [7] Nakamura R (2009): 3-D Attenuation structure beneath the Japanese Islands, source parameters and site amplification by simultaneous inversion using short period strong motion records and predicting strong ground motion, Doctoral Dissertation, The University of Tokyo, 2009. (in Japanese with English Abstract), <https://doi.org/10.15083/00002378>
- [8] Nakamura R, Shiina T (2019): Three-dimensional S-wave attenuation structure in and around source area of the 2018 Hokkaido Eastern Iwate Earthquake, Japan., *Earth Planets and Space*. <https://doi.org/10.1186/s40623-019-1095-6>
- [9] Nakamura R, Tsuruoka H, Kato A, Sakai S, Hirata N (2019): Effects of Underground Installation of Seismometers on Three Dimensional Attenuation Structure Inversion -Utilization of MeSO-net Data-, *The Journal of JAEE*, **20**(1), 1_1-1_12, https://doi.org/10.5610/jaee.20.1_1.
- [10] Borchardt RD (2002): Empirical evidence for acceleration-dependent amplification factors, *Bull. Seism. Soc. Am.*, **92**, 761-782. <https://doi.org/10.1785/0120010170>
- [11] Fujimoto K, Midorikawa S (2006): Relationship between Average Shear-Wave Velocity and Site Amplification Inferred from Strong Motion Records at Nearby Station Pairs, *The Journal of JAEE*, **6**(1), 11-22. <https://doi.org/10.5610/jaee.6.11>
- [12] Wessel P, Smith WHF (1998): New, Improved Version of Generic Mapping Tools Released, *EOS Trans.*, AGU, **79** (47), 579